Journal of Cellular Biochemistry 29:1–17 (1985)
Membrane Skeletons and Cytoskeletal-Membrane Associations 11–27

Structure of the Murine Anion Exchange Protein

Ron R. Kopito and Harvey F. Lodish

Whitehead Institute for Biomedical Research, Nine Cambridge Center (R.R.K., H.F.L.) and Department of Biology, Massachusetts Institute of Technology (H.F.L.), Cambridge, Massachusetts

A full-length clone encoding the mouse erythrocyte anion exchange protein, band 3, has been isolated from a cDNA library using an antibody against the mature erythrocyte protein. The complete nucleotide sequence has been determined. Substantial homology is evident between the deduced murine amino acid sequence and published sequences of fragments of human band 3 protein. The amino-terminal 420 and the carboxy-terminal 32 residues constitute polar, soluble domains, while the intervening 475 amino acids are likely to be intimately associated with the lipid bilayer. Hydrophobic analysis of this sequence, together with structural studies on the human protein, suggests the possibility of at least 12 membrane spans, predicting that both the amino- and carboxy-termini are intracellular.

Key words: erythrocyte plasma membrane, ion transport, membrane transport, anion exchange, band 3 protein

Band 3 is the major integral protein of the mammalian erythrocyte membrane, where it constitutes over 30% of the total protein [1]. Proteolytic mapping studies on erythrocytes and erythrocyte ghosts have identified two distinct structural and functional domains in this ~100,000-dalton glycoprotein. Trypsin digestion of ghosts or inside-out vesicles cleaves band 3 into a soluble N-terminal 41,000-dalton fragment (TR41) and a C-terminal 52,000-dalton membrane-associated fragment (TR52) [2]. TR41 constitutes a hydrophilic cytoplasmic pole that contains high-affinity binding sites for ankyrin [3,4], hemoglobin [5,6], and several glycolytic enzymes [7,8]. Via its attachment to ankyrin, band 3 serves to anchor the plasma membrane to the mesh-like network of spectrin and ankyrin, which constitutes the erythrocyte submembrane cytoskeleton (reviewed in [9]).

The membrane-associated domain (TR52) is responsible for the anion exchange activity of band 3, which mediates the physiological exchange of chloride and bicarbonate across the erythrocyte membrane. This process is a key step in the overall

Received March 19, 1985; revised and accepted May 20, 1985.

transport of carbon dioxide from respiring tissues to the lungs. The role of this exchange is shown in Figure 1. Within the capillaries, CO_2 readily diffuses into erythrocytes, where it is hydrated by carbonic anhydrase to form bicarbonate and a proton. The direction of this reaction depends on both the P_{CO_2} and on the efficient removal of the reaction products. The liberated proton binds to hemoglobin, thereby facilitating the release of oxygen (the Bohr effect), while the bicarbonate anion is exchanged for extracellular Cl^- by band 3. The one million molecules of band 3 on the surface of each erythrocyte [10] permit the rapid equilibration of the intracellularly formed bicarbonate with the extracellular aqueous space. Indeed, about 80% of the total carbon dioxide carried in the blood is in the form of bicarbonate anion dissolved in the water phases of erythrocytes and plasma [11]. All of the reactions shown in Figure 1 are reversed in the pulmonary circulation by high P_{O_2} and low P_{CO_2}. The anion exchange activity of band 3 has been extensively studied (reviewed in [12–14]). It behaves as a sequential process in which the transmembrane movement of anions is reversible, tightly coupled, and electrically silent.

Studies on the topology of the membrane-associated anion transport domain suggest that it traverses the membrane at least seven times [15,16]. Further proteolysis of TR52 with chymotrypsin results in its cleavage into 17-kD (CH17) and 35-kD (CH35) sub-fragments [2]. Interestingly, this proteolysis still results in no loss of anion exchange activity [17]. Digestion of intact erythrocytes with papain, however, which removes a 5-kD fragment from the N-terminus of CH35 and a few residues from the C-terminus of CH17 [15], dramatically alters the anion exchange process [18].

Investigations on the membrane-associated, anion exchange domain of band 3 (TR52) using proteolytic mapping, inhibitor binding, and covalent modification have permitted the identification of specific functional groups and domains of the protein that may be involved in the exchange process. Several models of anion exchange have been postulated that attempt to integrate the kinetic and biophysical data with the results of structural studies. Unfortunately, the intimate association with the lipid bilayer of the anion exchange domain of band 3 has hampered efforts to determine the sequence of all but two short fragments of this domain in the human protein. The

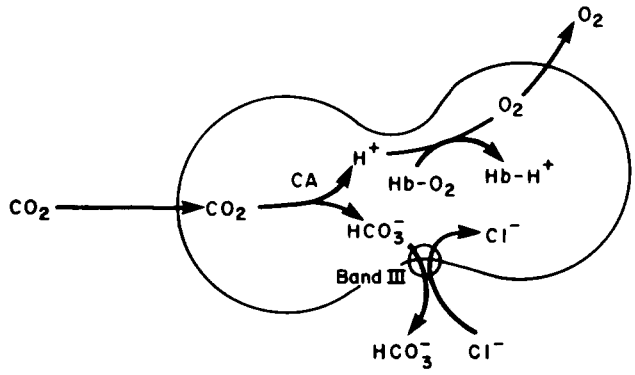

Fig. 1. The role of band 3 in CO_2 transport. Abbreviations used: CA, carbonic anhydrase; Hb, hemoglobin.

molecular mechanisms and the structural organization of this important protein have, therefore, remained enigmatic.

We have isolated and sequenced a full-length cDNA clone encoding the band 3 message from mouse [19]. Previous studies have established that human and mouse band 3 are very similar in both size and biochemical properties [20]. The amino acid sequence of band 3, deduced from the nucleotide sequence, allows us to design a testable model for protein-mediated transmembrane anion exchange. In this paper we discuss features of the amino acid sequence of the band 3 polypeptide deduced from the cDNA and propose a novel model for its transmembrane orientation and the possible spatial arrangement of its membrane-spanning regions, which incorporates data from the large number of biochemical and physiological studies on the human protein.

MATERIALS AND METHODS

Isolation of cDNA Clones and DNA Sequencing

Details of the construction of the cDNA libraries, antibody screening, and DNA sequence have been described elsewhere [19]. Briefly, a cDNA library from anemic mouse spleen RNA, in the expression vector λ-gt11 [21], was probed with a polyclonal antibody to mouse erythrocyte band 3 [20] and several partial-length cDNA clones were isolated. These were used to isolate the full-length cDNA from a size-selected λ-gt11 library. The complete nucleotide sequence [22,23] was obtained from the sequence of overlapping cDNA clones.

Computer-Assisted DNA Sequence Analysis

The sequence was compiled with the assistance of the programs of Staden [24]. Subsequent analysis of the sequence was performed using the ALIGN, RELATE, SEARCH, and DOTMATRIX programs [25], and the data base of Dayhoff et al [25].

Cell Culture

Friend murine erythroleukemia cells (MEL) [26] were maintained in culture as described [27]. Induction was achieved by incubating the cells in media containing 5% bovine serum albumin (BSA), 1.8% dimethylsulfoxide (DMSO) and 1.8 mM Imferon (Dow) as described [27].

RNA Blot Hybridization

RNA was prepared by disruption of the tissue in 5 M guanidinium isothiocynate, followed by centrifugation through a gradient of CsCl essentially as described [28]. Total RNA or poly(A)-enriched RNA [29] was separated on a 1.5% agarose gel containing 6% formaldehyde [30]. The RNA was transferred to a nylon filter and hybridized sequentially with nick-translated probes from mouse band 3 cDNA and rat α-tubulin cDNA [31]. Hybridization was performed in 5X SSC and 50% formamide at 42°C as described [30].

RESULTS

Mouse and Human Band 3 Share Sequence Homology

Figure 2 shows the complete sequence of 4,257 nucleotides compiled from overlapping cDNA clones. The size of the full-length cDNA agrees well with that of

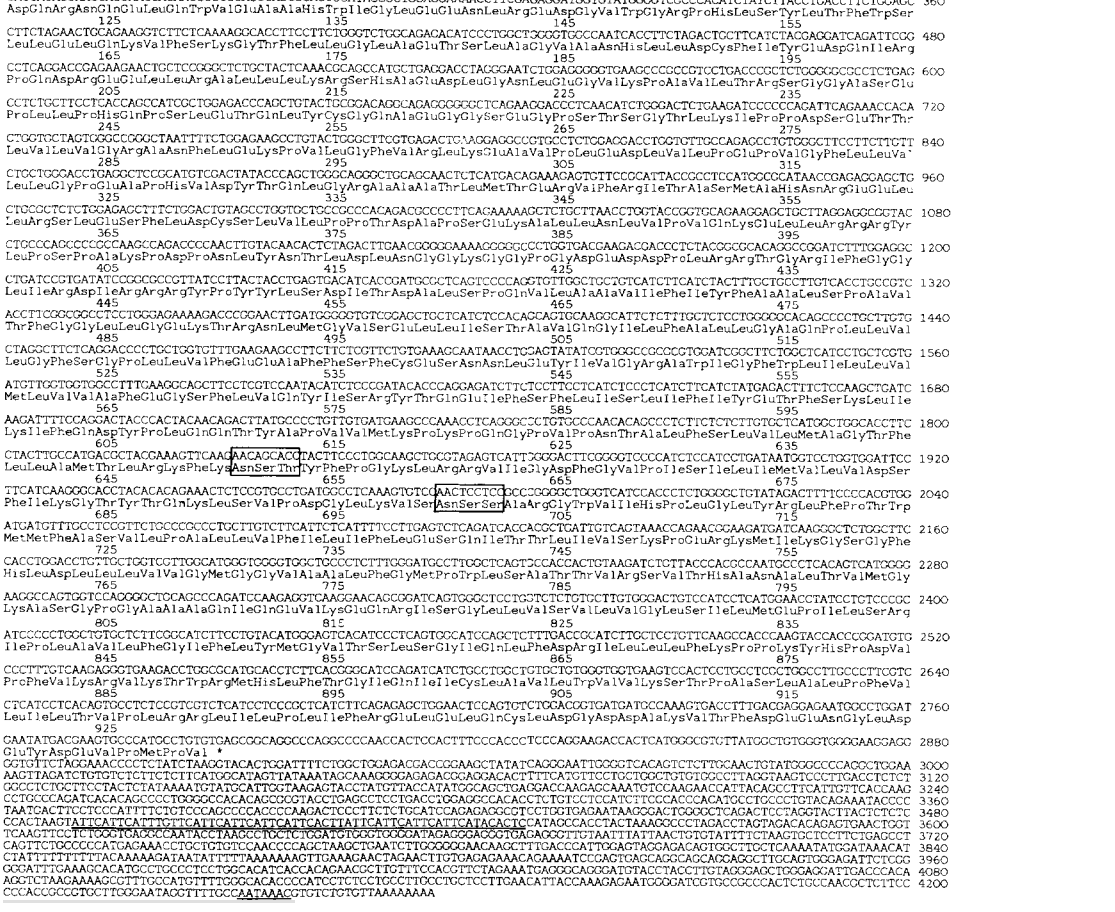

Fig. 2. Complete nucleotide sequence of band 3 cDNA showing deduced amino acid sequence. Nucleotide numbers are indicated in the right-hand margin, and the sequence is written with the 5′ end of the cDNA at the top left corner.

The in-frame nonsense codon at base −63 and an out-of-frame ATG at −50 are underlined. The two potential glycosylation sites at amino acids 611 and 660 are designated by boxes. Also underlined are the tandem repeat at nucleotide positions 3490–3550 and the polyadenylation signal at base 4232. Other relevant residues and structures are referred to in the text by number.

the mRNA (see Fig. 7). This sequence contains a single open reading frame (2919 bp) flanked by 127 bp and 1214 bp untranslated regions at the 5′ and the 3′ ends, respectively. The open reading frame extends for 929 codons from the ATG at nucleotide 1 to TGA at base 2919. There are two in-frame ATG codons at the beginning of the open reading frame (residues 1 and 4). We have assigned the first Met codon as the initiator because it is the first in-frame ATG downstream of the (in-phase) stop codon at base −63. The sequences flanking this ATG, but not the other,

are homologous to the highly conserved sequence that flanks functional initiation sites in eukaryotic mRNAs: AXX AUG G [29]. An out-of-frame ATG at position −50 is apparently not used, as it defines a reading frame of only 41 codons. The molecular weight of the predicted polypeptide is 103,000 daltons, in good agreement with estimates of 90,000–100,000 obtained from sodium dodecylsulfate (SDS)-polyacrylamide electrophoresis of the native human [1] and mouse [33] proteins. The predicted C-terminal amino acid of the mouse sequence is valine, which is also the C-terminal residue of the human protein [34]. Indeed, of the C-terminal 12 residues predicted from the mouse cDNA sequence, 11 are identical with those determined by carboxypeptidase-Y digestion of human band 3 [35]. Parts of the amino acid sequence deduced from the cDNA sequence are highly homologous to that of the several known fragments of human erythrocyte band 3 (Fig. 3), proving unequivocally that the clones we have isolated encode the mouse erythrocyte anion exchange protein.

The most striking homology is between residues 456 and 492 of mouse band 3 and the 38 amino acid fragment from the human protein designated H3 [36] in Figure 3. There is only a single conservative (leu → Val) substitution beteween the two sequences; there are no insertions or deletions. Excellent alignment is also observed between the deduced sequence of mouse band 3 and the sequence of a peptic fragment (P5) of the human protein designated H4 [37] (Fig. 3); only 5 of the 72 residues are different, and alignment of the sequences required no insertions or deletions. The sequence of the amino-terminal 201 residues of human band 3 [38], designated H1, also exhibits homology with the sequence deduced from the mouse band 3 clone. This homology is lower overall than either of the two C-terminal sequences discussed above.

Band 3 Has Three Structural Domains

A hydropathy plot [39] (Fig. 4) reveals that mouse band 3 can be roughly divided into three domains. The N-terminal 420 residues constitute the hydrophilic cytoplasmic domain with a decidedly negative net charge (65 acidic and 37 basic residues). The central region consists of 450 amino acids of mixed polar and apolar composition, and they are intimately associated with plasma membrane lipid. In this domain, groups of hydrophobic residues, which correspond to the peaks A–J in Figure 4, are interspersed with polar, predominantly basic, residues (Fig. 5). The third domain of band 3 encompasses the extreme 32 C-terminal residues. Eleven out of these are either glutamate or aspartate, making it unlikely that the C-terminus is buried within the lipid bilayer.

The Cytoplasmic Domain

The binding of hemoglobin [5,6] and glycolytic enzymes [7,8] to the cytoplasmic domain of human band 3 is mediated primarily by the first 11 residues of the band 3 polypeptide [5]. The total lack of homology between the mouse and human sequences in this N-terminal undecapeptide is consistent with the absence of detectable glyceraldehyde-3-phosphate dehydrogenase in mouse erythrocyte ghosts [40].

Low et al [41] proposed a domain structure for the cytoplasmic domain of band 3 in which the cytoplasmic domain is as homodimer with a "regulated hinge" rich in proline residues somewhere in the middle of CH65. These prolines apparently disrupt the α-helical conformation of the polypeptide in this region, rendering it more susceptible to proteolysis. It is noteworthy that these prolines (at positions 161, 188,

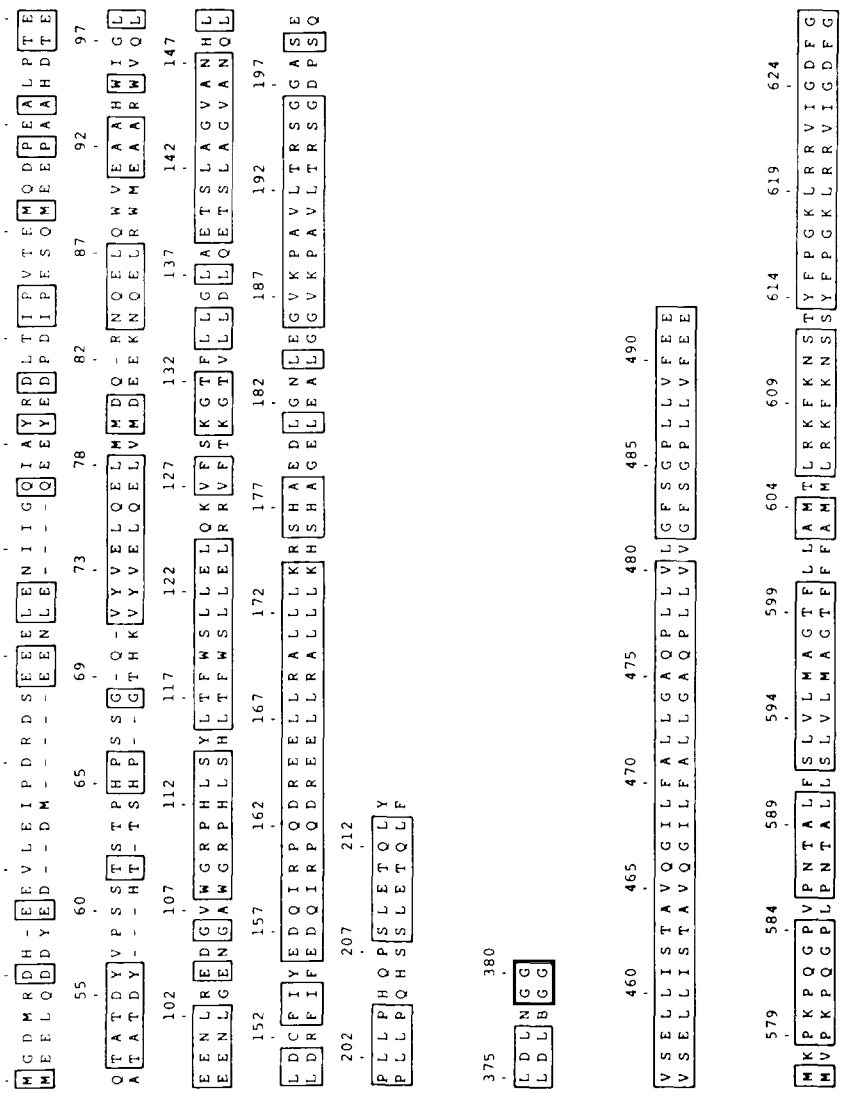

Fig. 3

201, and 204) are all conserved between human and mouse band 3 (cf Fig. 3); Figure 5 shows them to be clustered around a known trypsin cleavage site at position 194 [35]. (Interestingly, two other proline-rich regions in the predicted mouse sequence are found at the known primary sites of intracellular and extracellular proteolysis, between residues 361–368 and 567–586, respectively, Fig. 5) Between the proposed "hinge" and a region rich in tryptophan (residues 89–119), also highly conserved, is the purported antigenic region of band 3 [41]. Monospecific polyclonal antibodies against total human band 3 recognize determinants located within a 20-kD fragment of the cytoplasmic domain [42]; this site is sufficiently distant from the N-terminus so that the binding of antibody does not interfere with the binding of hemoglobin [41]. The region between residues 125 and 138 is only 57% homologous between human and mouse, while the residues flanking it on either side are 90–95% homologous. This observation is consistent with the lack of cross-reactivity of anti-human band 3 antisera with the mouse protein and vice versa [33].

The ankyrin binding site on band 3 has not been identified; Low et al tentatively place it between the "hinge" region and the "IgG" region, since antibodies against band 3 compete with labeled ankyrin for binding [41]. It is likely that the high-affinity ankyrin binding site is conserved among different species, and perhaps, among different nonerythroid ankyrin binding proteins. In Figure 5 we have tentatively positioned this binding site.

The Membrane-Associated Domain

Figure 4 indicates that the C-terminal ~500 amino acids are arranged in ten long hydrophobic stretches, labeled A–J. Regions of 20–24 amino acids with hydropathy averages exceeding 1.5 are usually tightly associated with lipid, and, in the case of several proteins, span the membrane in an α-helical configuration [39,43].

Examination of the band 3 sequence for potential membrane-spanning regions suggests that the regions corresponding to seven of the peaks in Figure 4 span the phospholipid bilayer once (A, C, D, E, F, G, H) and that two (B, I), and possibly a third (J), span twice. The putative membrane-spanning regions corresponding to these peaks have been numbered 1–12 as designated in Figure 5. We analyzed the sequences of these potential transmembrane segments by constructing helical "wheel diagrams" [44], assuming 3.6 amino acids per turn. These diagrams, examples of which are shown in Figure 6, have been used to predict amphipathic structures in other proteins [44]. One important observation from this analysis is that all of the potential membrane-spanning helices in band 3 (with the possible exception of helices 1 and 8) exhibit some degree of amphipathicity. In these helices, the amino acids bearing charged or polar side groups are all oriented toward a single face (Fig. 6b).

Band 3 Expression Is Regulated During Differentiation of (MEL) Cells

Figure 7 shows that pB33 hybridizes to a single species of RNA from anemic spleen cells that migrates in a denaturing agarose gel at 4.3 Kb. Friend erythroleukemia cells (MEL) [26] are induced to undergo terminal erythroid differentiation by

---

Fig. 3. Alignment of sequences of fragments of human band 3 with the deduced sequence of the mouse protein. Shown are the alignments for an N-terminal fragment, H1 (38), a short peptide from the N-terminus of a 14,000-dalton chymotryptic fragment, H2 (36), and two fragments from the membrane-associated domain, H3 (36) and H4 (37) (see Fig. 5 for their locations).

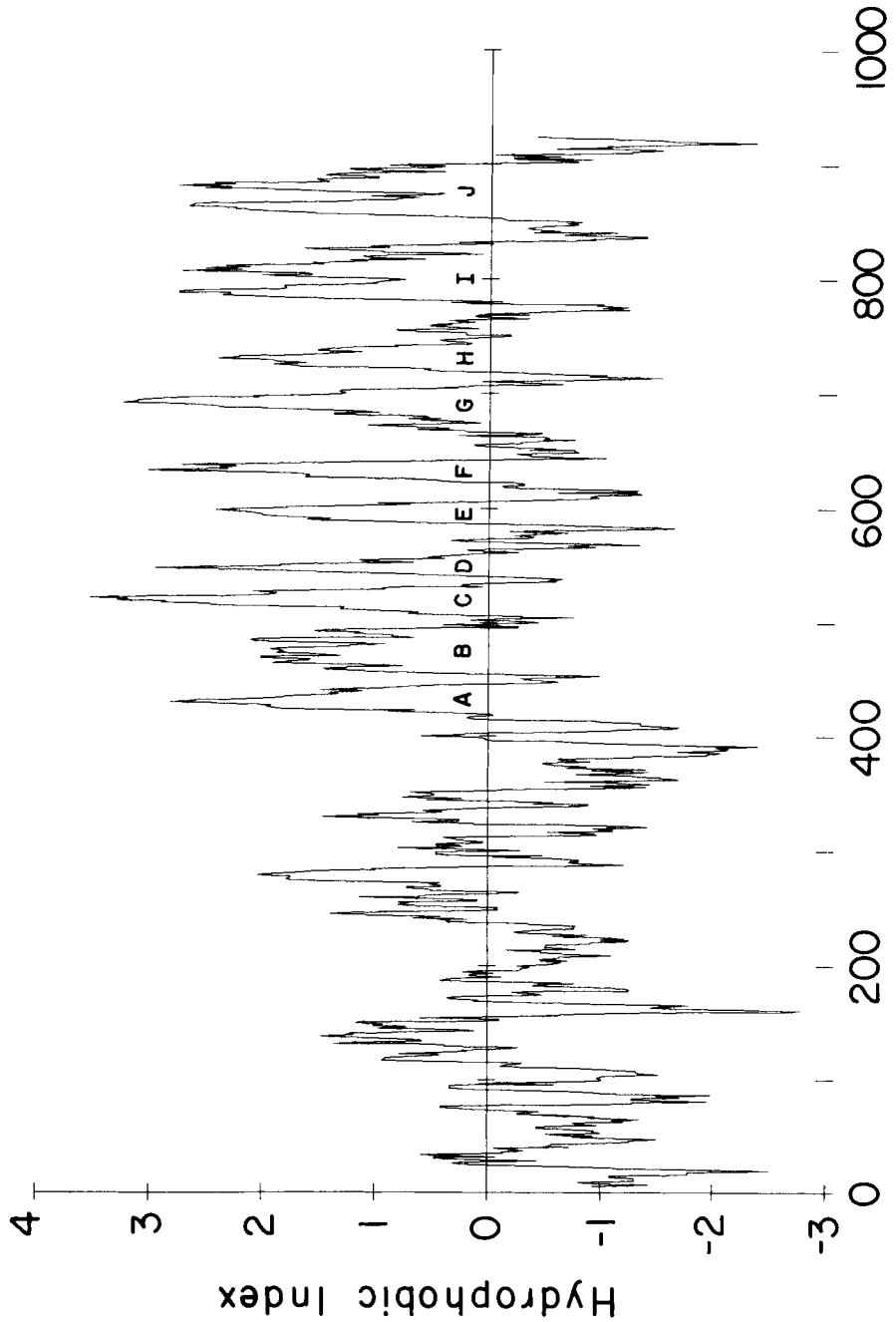
Hydrophobic Index
4
3
2
1
0
-1
-2
-3
0
200
400
600
800
1000
Residue Number
A
B
C
D
E
F
G
H
I
J

Fig. 4

treatment with DMSO or other agents [45]. Differentiation is accompanied by the accumulation of erythrocyte-specific mRNAs and the selective reduction in expression of nonerythroid genes [46]. Furthermore, induction of these cells results in the accumulation of several erythrocyte proteins including globin [46], band 3, and ankyrin [27,47]. Figure 7 shows that induction of MEL cells results in a significant increase in the level of band 3 mRNA and a concomitant loss of message for α-tubulin. The time course of the increase of band 3 RNA parallels the appearance of immunoprecipitable band 3 protein [27]. No additional bands were observable after overexposure (1 wk).

DISCUSSION

Transmembrane Orientation of the Band 3 Polypeptide

Figure 8 is a model for the proposed transmembrane orientation of the putative membrane-spanning regions of band 3. Chymotrypsin treatment of human erythrocytes cleaves band 3 into two fragments (CH65 and CH35) at a site corresponding to that in the mouse band 3 between membrane spans 5 and 6 [37]. Of the two potential sites (Asn-X-Ser/Thr) for attachment of the single N-linked oligosaccharide of band 3, the one at residue 611 corresponds to the site in the human protein shown by Brock et al [37] not to contain carbohydrate. Therefore, the site at Asn 660 must be the attachment site and thus must be extracellular. This analysis, taken together with the finding that the human Tyr 646 is a substrate for extracellular radioiodination [37], supports the conclusion that the region between helices 7 and 8 is extracellular.

The region encompassing segments 1 to 5 corresponds to part of the 17–22-kD chymotryptic fragment (CH17) that is generated by digestion of ghosts (Fig. 5). It must span the membrane an odd number of times since it results from both an intra- and an extracellular proteolytic cleavage [2]. Recent studies have demonstrated that this fragment traverses the bilayer a minimum of three times [16].

Assuming that peaks, A, C, and D of the hydrophobicity plot correspond to three membrane-spanning segments, 1, 4, and 5, then either region B (residues 453–491) does not span the membrane, or it must do so twice. The hydrophobicity peak B is quite broad, encompassing 38 moderately apolar residues. These residues can be arranged in a structure composed of two anti-parallel amphipathic helices with Pro 477 forming a turn within the membrane or just at the interface between the bilayer and the cytoplasm. Analysis of the helical amphiphilicity (Fig. 6b) suggests that both the helices formed by this region of the protein would have all their polar residues projecting from a single face of each helix. Thus, we conclude tentatively that CH17 possesses five membrane-spanning α-helices. This conclusion is further supported by the identification of the three lysine residues in CH17, which are accessible to extracellular impermeant labeling reagents (see below).

Virtually nothing is known about the transmembrane orientation of the C-terminus of band 3 corresponding to hydrophobic peaks G-J. Our model proposes four or five membrane crossings. The region corresponding to the 43 residues of peak I in Figure 4 resembles membrane spans 2 and 3 in its ability to form an

Fig. 4. Hydropathy plot of the deduced amino acid sequence of murine band 3. Hydrophobicites were averaged over windows of 11 amino acids. The residue number is plotted on the horizontal scale. The ten hydrophobic regions are designated A–J.

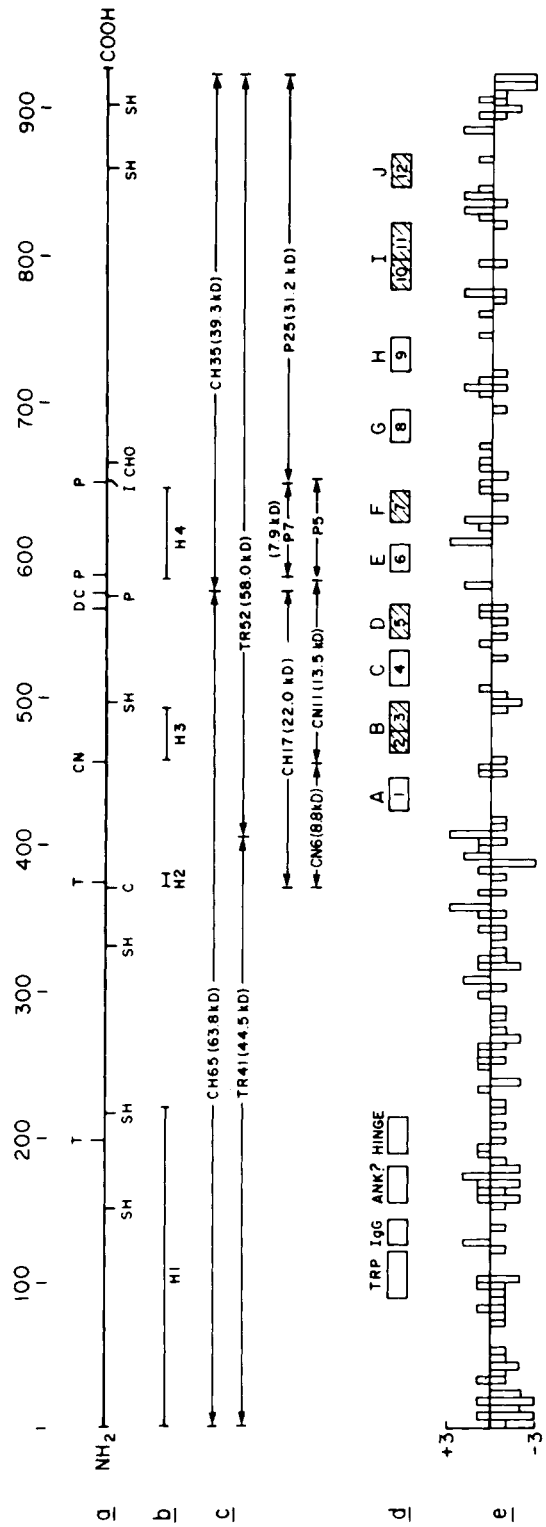
a
b
c
d
e
NH2
COOH
100
200
300
400
500
600
700
800
900
SH
T
C
CN
DC P
P
I CHO
H1
H2
H3
H4
CH65 (63.8 kD)
TR41 (44.5 kD)
TR52 (58.0 kD)
CH35 (39.3 kD)
CH17 (22.0 kD)
(7.9 kD)
P7
P25 (31.2 kD)
CN6 (8.8 kD)
CN11 (13.5 kD)
P5
A
B
C
D
E
F
G
H
I
J
TRP
IgG
ANK?
HINGE
+3
-3

Fig. 5

α-helical hairpin in which Arg 800 is situated just at the cytoplasmic surface and the C-terminal 24 amino acids return to the extracellular surface. The proline residues at positions 796 and 802 may be involved in forming the "hairpin" structure. These two spanning segments, along with #12, could form moderately amphipathic helices. Following an extremely polar stretch between residues 832 and 850, there is a short region of 18 mixed hydrophobic and polar residues that forms the N-terminal part of peak J in Figure 4. This is the longest stretch of apolar amino acids between position 850 and the C-terminus of the protein. Tentatively, we propose that this segment spans the membrane once, as an amphipathic α-helix (#12, Fig. 5). This would position the C-terminus of the protein inside the cell. Alternatively, the protein may traverse the membrane once more, leaving the C-terminus outside the cell (shown by the dotted lines in Fig. 8).

Location of the H_2DIDS-Binding Lysines in Band 3

Three lysines in human CH17 can be reductively methylated in intact cells by a membrane-impermeant reagent [16] and thus must be exofacial. Two of these are within the C-terminal CNBr fragment of human CH17; the third has been mapped to the N-terminal CNBr fragment of CH17 [16]. There are only three lysine residues in murine CH17 (at positions 449, 558, and 561). Given the high degree of homology between the human and mouse proteins in at least part of CH17 (H3), we assume that the positions of these lysine residues in human and mouse CH17 are the same.

One of the two lysines in the C-terminal CNBr fragment of human CH17 (CN11) is the one that binds extracellular 4,4′-diisothiocyano-2,2′ dihydrostilbene disulfonate (H_2DIDS), a bifunctional reagent that is a potent inhibitor of anion transport and a covalent crosslinker of CH17 and CH35 [48]. Segment #5 forms the C-terminus of mouse CH17. The helical wheel diagram shown in Figure 6b shows that segment #5 could form a membrane-spanning structure in which both Lys 558 and Lys 561 of mouse CH17 project near the extracytoplasmic surface of the membrane from the same side of an amphipathic α-helix together as the two acidic

---

Fig. 5. Domain map of band 3. a) The scale is the complete amino acid sequence of mouse band 3 deduced from the nucleotide sequence. Probable sites for proteolytic cleavage by trypsin (T) at position 194 (35) and 381 (36), chymotrypsin (C) (2), cyanogen bromide (CN) (16, 36), and Papain (P) (15) are indicated. Cysteine residues (SH) binding sites for H_2DIDS (D) and the known site for exofacial radioiodination (I) (32) are denoted. The proposed site for attachment of the N-linked oligosaccharide is designated (CHO). b) Alignment of the fragments from human band 3 is shown. The codes H1–H4 are defined in the legend to Figure 3. c) The predicted fragments arising from digestion of human band 3 with extracellular chymotrypsin, CH65 and CH35 (17, 34); intracellular trypsin, TR41 and TR52 (2); extracellular papain, P7 and P25 (15); extracellular pepsin, P5 (37); and cyanogen bromide cleavage of CH17, CN6, and CN11 (16, 36). The numbers in parentheses are the actual molecular weights of the fragments calculated from their amino acid composition. These values do not take into account the contribution of the single N-linked oligosaccharide. d) Structural features within the N-terminal cytoplasmic domain are as follows: tryptophan-rich (TRP) (41), antibody-binding (IgG) (41, 42), ankyrin-binding (ANK), and HINGE are indicated and are discussed in the text. The locations of the hydrophobic peaks from the hydropathy plot (Fig. 4) are indicated by the letters A–J, and the corresponding presumed membrane-spanning regions are designated by the numbers 1–12. Hatched boxes indicate that the region is likely to be amphipathic (see text for discussion). e) Charge plot. The location of charged residues in the mouse band 3 sequence is indicated by the bar graph, the positions corresponding to the sequence numbers are at the top of the figure. The basic residues (Arg and Lys) are assigned a value of +1 while the acidic residues (Glu and Asp) are assigned the value of −1. The bars represent the total (+) or (−) values, above and below the horizontal axis, respectively, as an average over five residues.

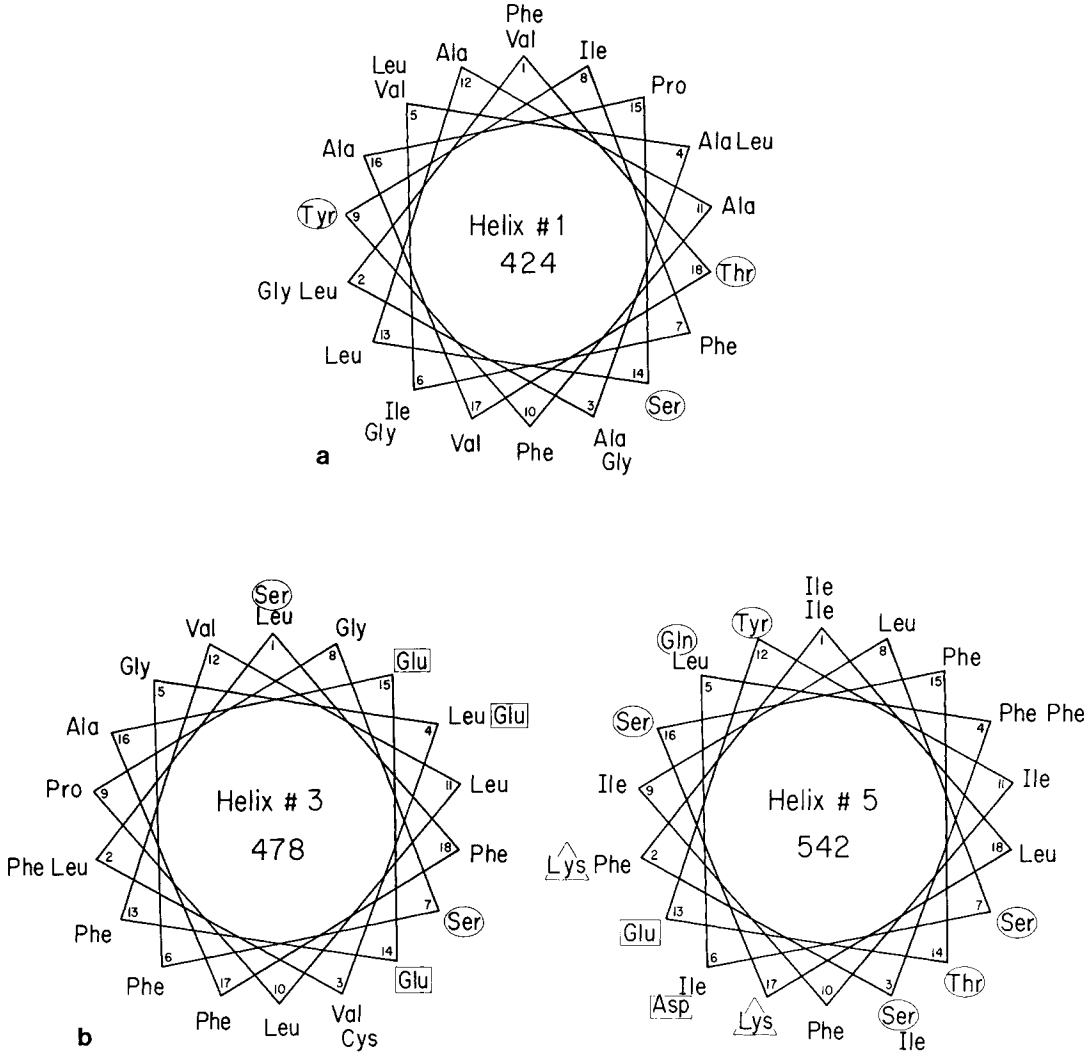

Fig. 6. Two-dimensional "wheel diagrams" of (a) helix #1 and (b) helices #3 and #5. Residues with polar, uncharged side chains are circled. Squares and triangles denote amino acids with acidic or basic side chains, respectively.

residues, Glu 554 and Asp 565. We therefore propose that the H_2DIDS-binding residue in CH17 is either Lys 558 or 561.

The remaining lysine in mouse CH17 is located near the N-terminus of the fragment (Lys 449). Since this residue is exofacial in human erythrocytes, it is likely that the Lys 449 in the mouse sequence must also face the extracytoplasmic surface, confirming that region A forms membrane-spanning domain #1 shown in Figures 5 and 6 (see above discussion).

The lysine residue in CH35, which is involved in the H_2DIDS crosslinking of this fragment to CH65, is located somewhere within the C-terminal papain fragment, P25 [5], which, in the mouse, contains 11 lysines. We speculate that one of the two between helices 7 and 8 (Lys 649 and 657) are involved in H_2DIDS crosslinking because of their proximity to the region of the protein where papain cleavage is associated with an alteration in anion transport.

The Structure and Mechanism of the Anion Exchange Site

Analysis of the predicted sequence of murine band 3 reveals that the protein possesses 12 potential membrane-spanning regions. Of these, five are quite hydrophobic and contain no residues withcharged side chains. The seven remaining membrane-spanning regions contain both hydrophobic, polar, and charged residues. We propose that the membrane-spanning regions of band 3 cross the plasma membrane in amphipathic helical structures that confine the polar and charged side chains to a single face of the helix. These helices, oriented with their axes transverse to the plane of the membrane, could cluster so as to form within the bilayer one or two hydrophilic regions in which the charged residues involved in the anion exchange process are allowed to pair and achieve a stable structure. Such clustering of amphipathic helices has been proposed for other transport proteins that span the membrane multiple times [49, reviewed in 43]. Significantly, the lysine residues that, we propose, bind to stilbene disulfonate inhibitors of anion exchange are associated with these amphipathic regions. The crosslinking of CH17 and CH35 by H_2DIDS suggests that these regions must be no more than 20 Å (the length of the H_2DIDS molecule) away from each other, despite the fact that they are separated by at least 80 amino acids. Identification of the H_2DIDS-binding lysine residue in P25 will be an important contribution to understanding the spatial arrangement of the membrane-spanning regions of band 3.

Band 3-mediated anion exchange activity has been described in terms of a sequential (ping-pong) mechanism involving the oscillation of the protein between two conformational states in which the anion binding site of each functional unit can exist at only one face of the membrane at any given time. An elegant model [12] proposes that pairing of an acidic and a basic residue within a positively charged cavity in the membrane forms an "anionic gate." Transport is initiated by the displacement of this charge pair by an exogenous anion and the formation of a new gate in the alternate conformational state. This hypothesis can account for the observed phenomena of substrate inhibition and "recruitment" of anion binding sites to a single side of the membrane [14].

All models of band 3-mediated anion exchange that have been proposed thus far have focused on the biochemistry and kinetics of this process and reflect the limitations imposed by the paucity of detailed structural information. In particular, these models have assumed that the anions are translocated through a single hydrophilic "channel" formed in the lipid bilayer by mono- or oligomeric band 3.

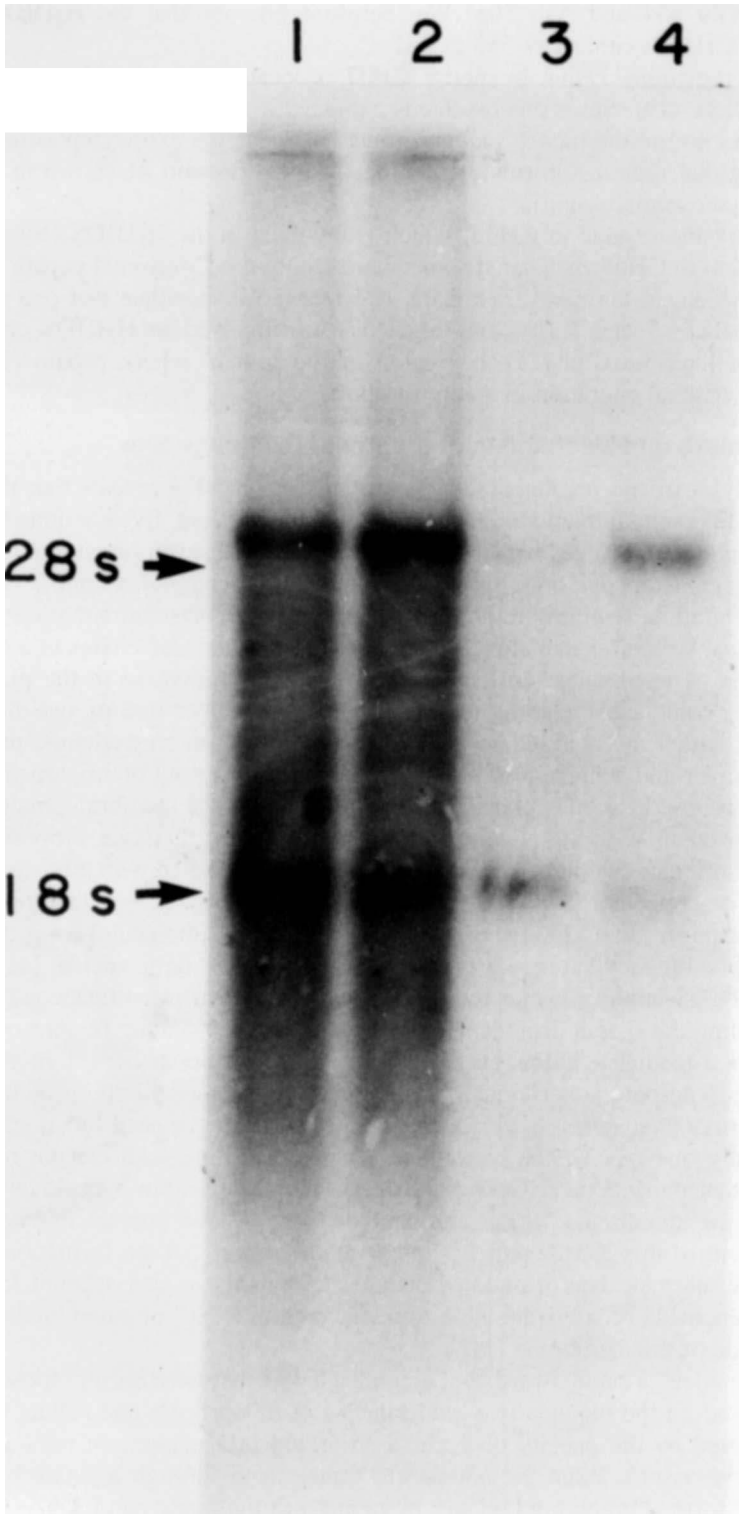

Fig. 7

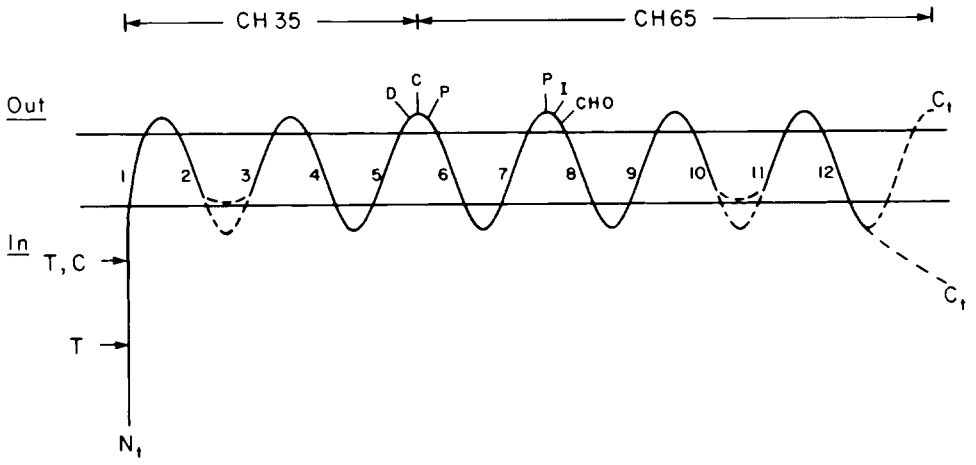

Fig. 8. A model for the proposed transmembrane orientation of band 3. Abbreviations are defined in the legend to Figure 5.

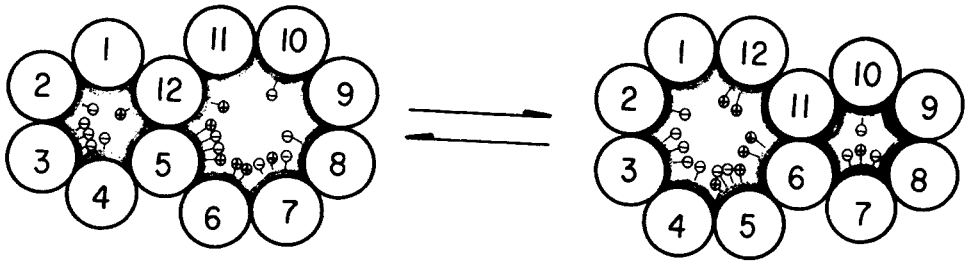

Fig. 9. A model for the arrangement of the membrane-spanning helices of band 3. The shaded area designates the polar faces of the amphipathic helices.

In Figure 9 we present a hypothetical structure for band 3 in which the hydrophilic faces of the 12 amphipathic helices of a single band 3 monomer are oriented to form the interiors of two separate channels. The protein could alternate between two conformational states as a consequence of the binding of an anion to a site at one face of the membrane. The affinity of the anion binding sites at the inner and outer faces of the membrane would be dependent upon the conformation.

This model may help to explain the tight coupling of inward and outward translocation steps in the exchange process and for the apparent involvement of both CH17 (helices 1–5) and CH35 (helices 6–12). Treatment of intact erythrocytes with papain, which cleaves the N-terminus of CH35 [48], specifically inhibits the outward

---

Fig. 7. RNA blot analysis of RNA from anemic mouse spleen and Friend erythroleukemia (MEL) cells. Lanes 1 and 2 contain total and poly(A^+) RNA from anemic mouse spleen, respectively. Lanes 3 and 4 contain poly(A^+) RNA from uninduced and 3-day induced MEL cells, respectively. The upper band results from hybridization of the blot with a mouse band 3 cDNA probe, while the lower band in each lane was obtained by reprobing the filters with a rat α-tubulin cDNA probe. The location of the 28s and 18s ribosomal bands are indicated as relative size markers.

translocation step of anion exchange while actually accelerating the inward process [18]. The structure of bacteriorhodopsin [50,51] suggests that seven membrane spans appear to be sufficient to form a channel for the vectorial translocation of a single ion. It is intriguing that CH17, embedded in lipid bilayers, appears to behave as a DIDS-sensitive, voltage-dependent chloride channel [52].

Our model is presented here as an alternative to previously described models that, implicitly and explicitly, have envisioned a single passageway through which anions can cross the membrane. It remains to be determined whether our model can account for all of the kinetic and biophysical data. Most importantly, however, several features of the structure proposed in Figure 9 are testable. The loops that, on both sides of the membrane, connect the membrane-spanning regions are rich in basic amino acids. At least Lys 558 and 561 and probably others may form part of the anion binding domain. It will be of interest to individually mutate these and other lysine residues; such mutations could alter the activity of the protein and/or cause it to accumulate in one of two conformational states. Such studies are in progress and could contribute to our understanding of the molecular biology of anion transport.

ACKNOWLEDGMENTS

We thank V. Patel for advice on the MEL cell cultures and G. Natsoulis and M. Kreitman for assistance with DNA sequencing. We are grateful to S. Alper, R. Doolittle, M. Jennings, J. Kyte, A. Garcia, and R. Reithmeier for helpful discussions. This work was supported by grant No. PO1-HL-27375 from the NIH. R.R.K. is supported by NIH postdoctoral grant No. F32 HL06680. We also thank Miriam Boucher for help with the manuscript.

REFERENCES

1. Fairbanks G, Steck TL, Wallach DFH: Biochemistry 10:2606, 1971.
2. Steck TL, Ramos B, Strapazon E: Biochemistry 15:1153, 1976.
3. Bennett V, Stenbuck PJ: Nature 280:468, 1979.
4. Bennett V, Stenbuck PJ: J Biol Chem 255:6424, 1980.
5. Walder JA, Chatterjee R, Steck TL, Low PS, Musso GF, Kaiser ET, Rogers PH, Arnone A: J Biol Chem 259:10238, 1984.
6. Shaklai N, Yguerabide J, Ranney HM: Biochemistry 16:5593, 1977.
7. Strapazon E, Steck TL: Biochemistry 15:1421, 1976.
8. Yu J, Steck TL: J Biol Chem 250:9176, 1975.
9. Bennett V: J Cell Biochem 18:49, 1982.
10. Steck TL: J Cell Biol 62:1, 1974.
11. Weith JO, Andersen OS, Brahm J, Bjerrum PH, Borders CL: Philos Trans R Soc Lond B299:383, 1982.
12. Macara IG, Cantley LC: In Elson E, Frazier W, Glaser L (eds): "Cell Membranes, Methods and Reviews." New York: Plenum Press, 1982, pp 41–87.
13. Cabantchik ZI, Knauf PA, Rothstein A: Biochim Biophys Acta 515:239, 1978.
14. Knauf PA: Curr Top Membrane Transport 912:249, 1979.
15. Jennings ML, Lackey MA, Denney DH: J Biol Chem 259:4652, 1984.
16. Jennings ML, Nicknish JS: Biochemistry 23:6432, 1984.
17. Grinstein S, Ship S, Rothstein A: Biochim Biophys Acta 507:294, 1978.
18. Jennings ML, Adams MF: Biochemistry 20:7118, 1981.
19. Kopito RR, Lodish HF: Nature 316:234, 1985.
20. Braell WA, Lodish HF: J Biol Chem 256:11337, 1981.
21. Young RA, Davis RW: Proc Natl Acad Sci USA 80:1194, 1983.

22. Maxam A, Gilbert W: Meth Enzymol 65:499, 1980.
23. Sanger F, Nicklen S, Coulson AR: Proc Natl Acad Sci USA 74:5463, 1977.
24. Staden R: Nucl Acids Res 10:4731, 1982.
25. Dayhoff MO, Barker WC, Hunt TL: Methods Enzymol 91:534, 1983.
26. Friend C, Scher W, Holland JG, Sato T: Proc Natl Acad Sci USA 68:378, 1978.
27. Patel VP, Lodish HF: Science 224:996, 1984.
28. Chirgwin JM, Przybyla AE, McDonald RJ, Rutter WJ: Biochem 18:5294, 1979.
29. Aviv H, Leder P: Proc Natl Acad Sci USA 69:1408, 1972.
30. Maniatis T, Fritsch EF, Sambrook J: "Molecular Cloning: A Laboratory Manual." New York: Cold Spring Harbor, 1982.
31. Lemishka IR, Farmer S, Rocaniello VR, Sharp PA: J Mol Biol 51:101, 1981.
32. Kozak M: Nucleic Acids Res 9:5223, 1981.
33. Braell WA: PhD dissertation, Massachusetts Institute of Technology, 1981.
34. Drickamer LK: J Biol Chem 251:5115, 1976.
35. Reithmeier R: Personal communication.
36. Mawby WJ, Findlay JBC: Biochem J 205:465, 1983.
37. Brock CJ, Tanner MJA, Kempf C: Biochem J 213:577, 1983.
38. Kaul RK, Murthy PSN, Reddy AG, Steck TL, Kohler H: J Biol Chem 258:7981, 1983.
39. Kyte J, Doolittle RF: J Mol Biol 157:105, 1982.
40. Patel V: Personal communication.
41. Low PS, Westfall MA, Allen DP, Appell KC: J Biol Chem 259:13070, 1984.
42. England BJ, Gunn RB, Steck TL: Biochim Biophys Acta 623:171, 1980.
43. Eisenberg D: Annu Rev Biochem 53:595, 1984.
44. Schiffer M, Edmundson AB: Biophys J 7:121, 1967.
45. Marks PA, Rifkind RA: Annu Rev Biochem 47:419, 1978.
46. Eisen H, Bach R, Emery R: Proc Natl Acad USA 74:3898, 1977.
47. Sabban EL, Sabatini DD, Marchesi JT, Adesnik M: J Cell Physiol 104:261, 1980.
48. Jennings ML, Pasow H: Biochim Biophys Acta 554:498, 1979.
49. Finer-Moore J, Stroud RM: Proc Natl Acad Sci USA 81:155, 1984.
50. Henderson R, Unwin PNT: Nature 257:23, 1925.
51. Khorana HG, Gerber GE, Herlihy WC, Gray CP, Anderegg RJ, Nihei K, Biemann K: Proc Natl Acad Sci USA 76:5046, 1979.
52. Galvez LM, Jennings ML, Tosteson MT: Fed Proc 43:315, 1984.